Design and Measurement of a 2x2 Array of Coaxial Periodic Leaky-Wave Antennas

Syed Osama Kamal and Lai Bun Lok
Department of Electronic and Electrical Engineering, University College London, London, UK, syed.kamal@ucl.ac.uk

***Abstract*—A 2x2 array of coaxial periodic leaky-wave antennas at X-band has been designed, fabricated and measured. It achieved a gain of more than 10 dBi at 9.8 GHz, input return loss better than 10 dB from 8 GHz to 12 GHz (other than the broadside frequency) and a 3 dB beamwidth of 9 degrees. The sidelobe level is better than 10 dB from 8 GHz to 10.5 GHz. The antenna also achieved a reduced open stopband attenuation at 9.8 GHz. A beam scanning range of 35 degrees from backward to forward direction over a 4 GHz span was achieved. Good agreement between the simulated and measured results was obtained.**

***Index Terms*—leaky-wave antenna, slotted waveguide array, radar.**

I. Introduction

Leaky-wave antennas (LWA) have been the subject of interest due to their unique radiation characteristics of frequency beam scanning, simple feed network and narrow beamwidths [1][2]. One type of leaky-wave antenna is the periodic LWA, which scans their beam as a function of frequency [3][4]. When implemented using coaxial cable, the LWA possesses compact size and is relatively easy to deploy [5][6]. These features make coaxial periodic leaky-wave (CPLW) antennas suitable for imaging and radio communications [7][8], radar antennas [9][10], wide bandwidth aerial communications [11] and weather/surveillance monitoring systems [12].

However, there are two main drawbacks that affect the performance of a CPLW antenna: (i) an open stopband attenuation, which results in a gain reduction at broadside frequency [13] causing a non-linear gain frequency response, and (ii) their overall longer length, particularly at RF frequencies below a few GHz [14]. Researchers have investigated methods to eliminate the open stopband attenuation, including the use of radiating stubs [15] and tapered slots [16] to suppress the open bandstop region. Reducing the cable length required for a conventional CPLW antenna featuring a wide beam scanning range poses a significant challenge at lower frequencies, owing to the periodicity and number of slots required.

In this work, we investigate the use of four shorter, periodically etched semi-rigid coaxial cables to form a 2x2 CPLW antenna array at X-band. Compared to conventional CPLW antennas, the proposed CPLW antenna array yields a narrow directive beam with low sidelobe and backlobe levels and overall gain exceeding 10 dBi from 8.5 GHz to 11.5 GHz. Due to the four-fold reduction in overall length compared to a conventional CPLW antenna, the 2x2 CPLW antenna array could be deployed more easily.

II. Design and Parametric Analysis

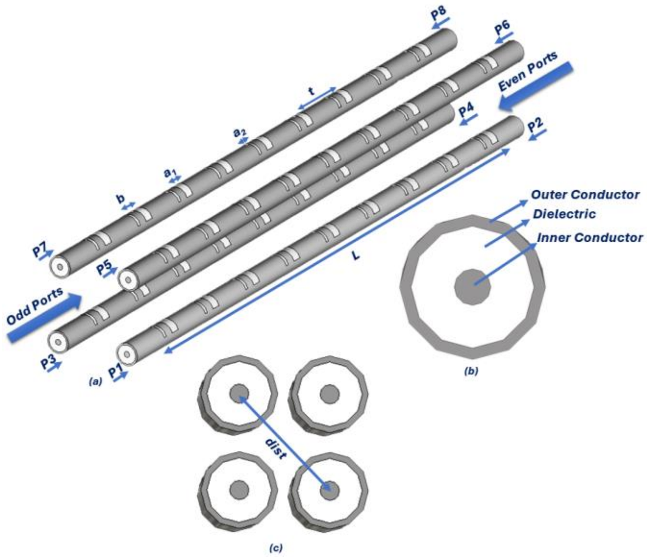

Fig. 1. Structural parameters of the 2x2 CPLW antenna array

A. Design

Fig. 1 shows the structure of the 2x2 CPLW antenna array. It consists of four identical (semi-rigid) coaxial cables each with an inner conductor diameter of 1.66 mm, outer conductor diameter of 6.3 mm and an insulating dielectric with ε_r of 2.05. Slots are etched on the outer conductor of the coaxial cable. The periodicity of these slots form space harmonics of the *n*-th order, which can be written as:

$$\beta_n = \beta_0 + 2n\pi/p \qquad (1)$$

where p is the slot period and β_n is the phase constant of the n-th harmonic. To calculate the slot period, the guided wavelength λ_g is computed as 20.7 mm at 10 GHz by:

$$\lambda_g = c/f\sqrt{(\varepsilon_r)} \qquad (2)$$

where c is the speed of light in freespace, f is the operating frequency and ε_r is the relative permittivity of the cable dielectric. The periodic slots are truncated on the cable by the guided wavelength distance and the required cable length L is also dependent on the operating guided wavelength:

$$\alpha/k_0 = 0.18\times\lambda_g/L \qquad (3)$$

where $k_0 = 2\pi/\lambda$. Since four cables are used, L = 200 mm has been chosen, accommodating nine identical slots on each cable [17]. The slot dimensions are denoted as a_1 for the wide slot, a_2 for the narrow slot and d is the distance between the wide and narrow slots pair. Each slot depth is 2.35 mm. The four cables were equispaced with separation of $dist = \lambda_g$ as shown in Fig. 1 as a 2x2 array to produce a broadside beam [18].

B. Parametric Analysis

Two sets of excitation ports herein named *Odd Ports* and *Even Ports* are used to feed the antenna array. As shown in Fig. 1(a), the *Odd Ports* are excited from the left hand side closest to the first narrow slot. The lower pair of CPLW antenna ports are designated P1 and P3, and the upper pair of CPLW antenna ports are designated P5 and P7. Alternatively, the *Even Ports* are excited from the right hand side that is closest to the first wide slot. In this case, the lower pair of CPLW antenna ports are designated P2 and P4, while the upper pair of CPLW antenna ports are designated P6 and P8. Any unexcited ports are terminated with 50 Ω loads. All four CPLW antennas are placed at 20.7 mm from the centre point of their signal conductors, as shown in Fig 1(c). The input ports are excited differentially with equal amplitude. The lower port pair of the antenna array can be fed differentially while the upper port pair of the antenna array can be fed in-phase, or vice-versa.

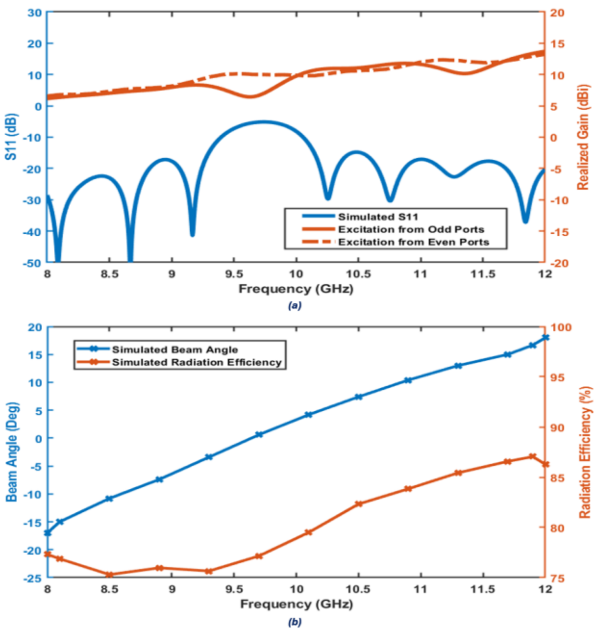

Fig. 2. (a) Simulated $|S_{11}|$ and realized gain of 2x2 CPLW antenna array (optimal values), (b) main radiated beam angle versus frequency.

In Fig. 2, it is evident that exciting the array from the *Odd Ports* results in lower open stopband attenuation compared to excitation from the *Even Ports*. While the input return loss demonstrates good characteristics at the broadside frequency, the open stopband attenuation experiences a reduction of approximately 5 dB when the array is excited from the *Even Ports*. The realized gain is generally linear from 8 GHz to 12 GHz. The size of the 2x2 CPLW antenna array is 26.5 mm x 26.5 mm x 200 mm.

The radiation pattern of this 2x2 CPLW antenna array demonstrates enhanced directivity and a reasonable front-to-back ratio at the broadside frequency, as illustrated in Fig. 3.

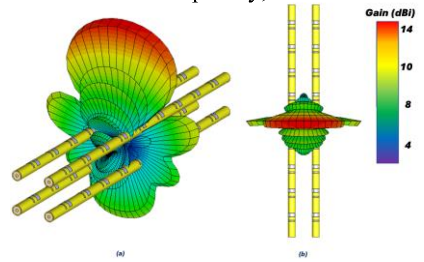

Fig. 3. Radiation pattern at 9.8 GHz (a) perspective view, (b) top view.

A parametric study was performed by varying the parameters a_1, a_2 and b. From Fig. 4(a) and 4(b), varying b from 0.016λ (1 mm) to 0.163λ (5 mm) improved the input return loss by 5 dB at 9.8 GHz. Here, λ is the freespace wavelength at 9.8 GHz. The antenna gain improved by 3 dB when b was varied from 1 mm to 5 mm. From Fig. 4(d), the design showed a similar trend when a_1 was varied from 0.049λ (1.5 mm) to 0.147λ (4.5 mm). The overall gain was improved by approximately 3 dB from 8 GHz to 12 GHz. However, the change in broadside frequency gain was less significant. When a_2 was varied from 0.016λ (0.5 mm) to 0.098λ (3.0 mm), the realized gain was improved by 5 dB as shown in Fig. 4(c). The optimal values for a_1, a_2 and b were found to be 0.098λ (3 mm), 0.033λ (1 mm) and 0.098λ (3 mm) respectively.

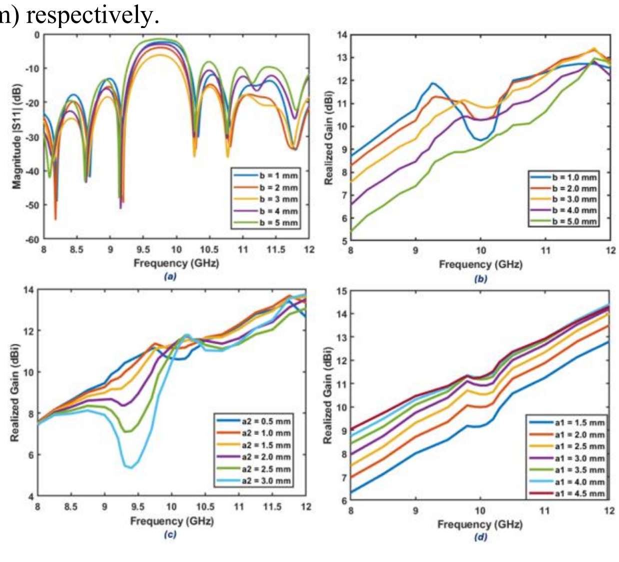

Fig. 4. Parametric results for: varying b on (a) $|S_{11}|$ and (b) realized gain with a_1 = 3 mm and a_2 = 1 mm; varying a_1 and a_2 (c) and (d) gain variation with b = 3 mm.

III. Fabrication and Measurement

A. Fabrication

Four 225 mm long semi-rigid coaxial cables were etched with nine wide slots of a_1 = 3 mm and nine narrow slots of a_2 = 1 mm over a length of 200 mm. A manual milling machine and fixed Dremel tool were used to manually etch the coaxial cables. In-line SMA connectors were soldered at each cable end.

To feed the 2x2 CPLW antenna array, a wideband 4-way power divider was realised on PCB as shown in Fig. 5. Isolation resistors of 100 Ω were used for R1, R2 and R3. The PCB substrate (Taconic TSM-DS3) has a thickness of 0.25 mm and ε_r of 3. The power divider splits the input power with a phase difference of 180° for two input ports and 0° for the other two input ports. This is achieved by extending the electrical length of the other two ports at 9.8 GHz with respect to the electrical length of the input port. In this way, the power divider acts as a Wilkinson power divider for in-phase split for two ports, and anti-phase split for the other ports.

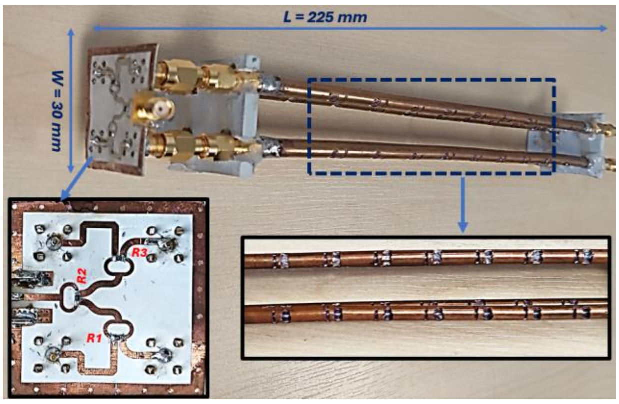

Fig. 5. Fabricated antenna fed with 1-to-4 power divider.

B. Measurement

The 2x2 CPLW antenna array was measured in an anechoic chamber with a vector network analyser to evaluate the antenna radiation pattern and realized gain characteristics. A reference horn antenna was used while the 2x2 CPLW antenna array was rotated around the *z*-axis to measure the radiation pattern from 8 GHz to 11 GHz. The far-field radiation patterns of the 2x2 CPLW antenna array were measured in the *y*-*z* plane (Phi=0°) with theta scans from -90° to +90° in 1° steps.

Additionally, Fig. 6(b) shows a setup involving movement of a reference horn antenna while keeping the 2x2 CPLW antenna array position fixed was devised to demonstrate the target detection performance of the array. The frequency response of $|S_{21}|$ was measured as the reference antenna is moved in discrete steps from a downward to upward position. The separation distance between the 2x2 CPLW antenna array and the reference horn antenna was manually adjusted from 80 cm to 160 cm in three incremental steps, as illustrated in Fig 6.

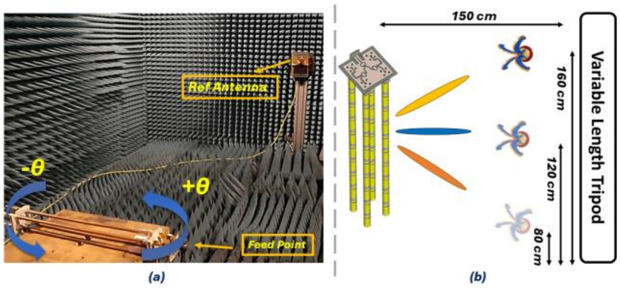

Fig. 6. Measurement setup for (a) radiation pattern, and (b) recording $|S_{21}|$

IV. Results and Discussion

Fig. 7 shows the simulated and measured input reflection coefficients and realized gains. Discrepancies between the simulated and measured results can be attributed to practical fabrication tolerances. The realized gain is linear over the frequency band of 8 GHz to 12 GHz with no open stopband attenuation. 10 dBi gain was measured from 9 GHz to 10.75 GHz. The parabolic gain curve over the entire bandwidth is due to phase imbalance of the power divider above and below 9.8 GHz. Therefore, the power divider is non-ideal below 9 GHz and beyond 10.75 GHz, causing a gradual reduction in gain. The power divider imperfections also affect the sidelobe level which increases above 10.5 GHz. The sidelobe level is less than -10 dB at 9.8 GHz.

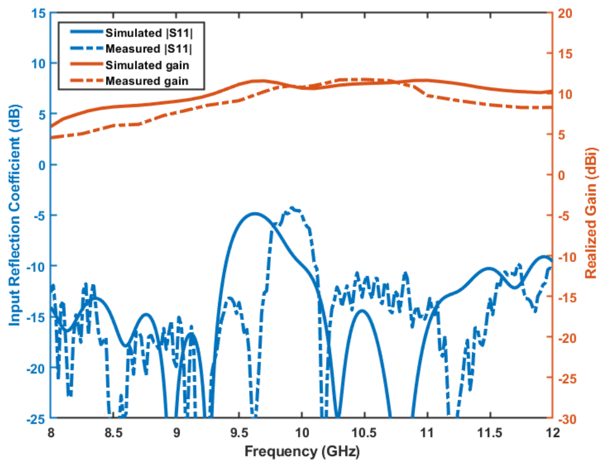

Fig. 7. Simulated and measured $|S_{11}|$ and gain.

The normalized far field radiation patterns are shown in Fig. 8. The simulated far field radiation angle from 8 GHz to 12 GHz is found to be -17° to +18°, respectively. The 2x2 CPLW antenna array shows a good linear gain response versus frequency, with more than 35° of scanning range from backward to forward direction.

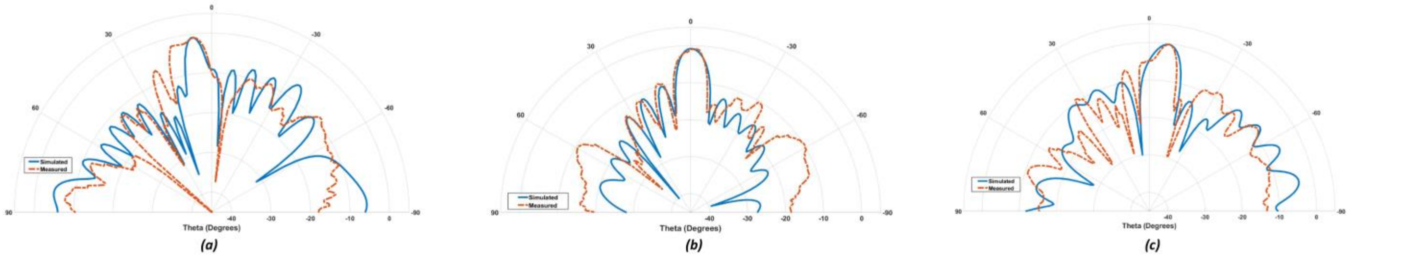

Fig. 8. Farfield radiation patterns at (a) 10.5 GHz, (b) 9.8 GHz and (c) 8.5 GHz

To illustrate the use of the proposed antenna in a beam scanning application, we conducted an experiment involving the 2x2 CPLW antenna array vertically mounted at 150 cm from a reference horn antenna, which was manually moved to 80 cm, 120 cm and 160 cm above the ground. For each configuration, the 2x2 CPLW antenna array was fed from an upward direction and $|S_{21}|$ was measured from 8 GHz to 12 GHz. The results demonstrated successful target detection at: 8.7 GHz for 160 cm, 9.8 GHz for 120 cm, and 10.9 GHz for 80 cm. Notably, the signal levels were consistently more than 7 dB below the peak $|S_{21}|$ of the target. This capability holds significant value for acquiring radar profile data without the need to move the 2x2 CPLW antenna array, making it potentially useful for borehole radar applications.

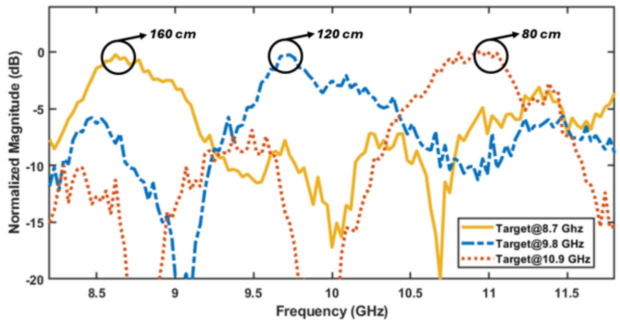

Fig. 8. Normalised |S21| frequency response for target detection

Table I shows the performance of LWAs implemented with an array of coaxial cables compared to LWA implementations using other transmission line media. The proposed 2x2 CPLW antenna array offers a reduced size and high gain at broadside frequency.

TABLE I. COMPARISON OF RELATED LEAKY-WAVE ANTENNA ARRAYS

Ref.	Freq. (GHz)	Broadside realized gain	Scan angle	Width	Trans. Line Media
[19]	14.6 - 15.6	5 dBi (15 GHz)	13°	$1.5\lambda_o$	SIW
[20]	3.8 - 4.1	10.1 dBi (3.9 GHz)	n/a	$2.96\lambda_o$	Microstrip
[21]	55.0 - 65.0	10.1 dBi (60 GHz)	60°	$7\lambda_o$	Meta-material
This work	8.0 - 12.0	10.6 dBi (9.8 GHz)	35°	$0.98\lambda_o$	Coaxial

V. CONCLUSION

A 2x2 CPLW antenna array has been demonstrated and shows a potential for beam scanning target detection. The beam scanning capability is achieved through a simple circuit design and offers advantages for deployment in remote and resource-constrained areas. It obviates the need to manually position the measurement antenna. Our proposed design also caters to applications with restricted spatial constraints, where antenna size can only be extended along one axis.

The proposed antenna provides a gain of more than 10 dB at 9.8 GHz, a fractional bandwidth of 40% with a -3 dB beamwidth of approximately 10° and a scanning range of 35° from backward to forward direction over the 8 GHz to 12 GHz band. The 2x2 CPLWA array is compact and yields a more directive beam compared to conventional CPLWAs. Importantly, it exhibits no open stopband attenuation at the broadside frequency.

Designing compact CPLWA arrays for lower frequencies will be more challenging due to the longer guided wavelengths. Ongoing work is investigating a scaled adaptation of the proposed 2x2 CPLWA array concept for operation within the UHF/L-bands aimed at borehole geophysical radar applications.

ACKNOWLEDGMENT

S. O. K. and L. B. L. thank Martin Scott for fabricating the PCB. This work was supported by the Royal Society (URF\R\201040).

REFERENCES

[1] Y. Ma, J. Wang, Z. Li, Y. Li, M. Chen, and Z. Zhang, "Planar annular leaky-wave antenna array with conical beam," *IEEE Transactions on Antennas and Propagation*, vol. 68, no. 7, pp. 5405–5414, 2020.

[2] Y. Geng, J. Wang, Y. Li, Z. Li, M. Chen, and Z. Zhang, "A Ka-band leaky-wave antenna array with stable gains based on HMSIW structure," *IEEE Antennas and Wireless Propagation Letters*, vol. 21, no. 8, pp. 1597–1601, Aug. 2022.

[3] A. K. Tiwari, S. Awasthi, and R. K. Singh, "A symmetrical periodic leaky-wave antenna with backward-to-forward scanning," *IEEE Antennas and Wireless Propagation Letters*, vol. 19, no. 4, pp. 646–650, 2020.

[4] A. Zandamela, A. Al-Bassam, and D. Heberling, "Circularly polarized periodic leaky-wave antenna based on dielectric image line for millimeter-wave radar applications," *IEEE Antennas and Wireless Propagation Letters*, vol. 20, no. 6, pp. 938–942, 2021.

[5] Y. Nasirudeen, M. K. Mandal, and R. Shaw, "Circularly polarized high gain coaxial line leaky wave antenna with backfire radiation," *IEEE Transactions on Antennas and Propagation*, vol. 70, no. 5, pp. 3824–3827, 2022.

[6] J. Lu, J. Geng, K. Wang, S. Yang, R. Zhao, X. Tang, D. Su, A. Zhang, and H. Li, "A wideband circularly polarized periodic leaky-wave antenna using a novel unit cell with X-shaped slot," *IEEE Transactions on Antennas and Propagation*, vol. 71, no. 8, pp. 6639–6651, Aug. 2023.

[7] M. S. Rabbani, J. Churm, and A. Feresidis, "Millimetre-wave beam steerable leaky-wave antenna for 5G systems," in *12th European Conference on Antennas and Propagation,* 2018, pp. 1–4.

[8] J. S.-T, Yang and H. Ling, "Application of compressive sensing to two dimensional radar imaging using a frequency-scanned microstrip leaky wave antenna," *Journal of Electromagnetic Engineering and Science*, vol. 17, no. 3, pp. 113–119, 2017.

[9] D. K. Karmokar and Y. J. Guo, "Planar leaky-wave antennas for low cost radar," in *IEEE-APS Topical Conference on Antennas and Propagation in Wireless Communications*, 2017, pp. 112–115.

[10] J. Tebart, M. Steeg, and A. Stohr, "Photonics-based FMCW radar localization using direct laser modulation and leaky-wave antenna beam scanning," in *45th International Conference on Infrared, Millimeter, and Terahertz Waves*, 2020, pp. 1–2.

[11] J. L. Gomez-Tornero, *Smart Leaky-Wave Antennas for Iridescent IoT Wireless Networks*. John Wiley & Sons, 2022, ch. 4, pp. 119–181.

[12] Y. Yuan and C.-T. M. Wu, "Recent development of non-contact multi-target vital sign detection and location tracking based on metamaterial leaky wave antennas," *Sensors*, vol. 21, no. 11, 2021.

[13] S. Rezaee and M. Memarian, "Analytical study of open-stopband suppression in leaky-wave antennas," *IEEE Antennas and Wireless Propagation Letters*, vol. 19, no. 2, pp. 363–367, 2020.

[14] L. Shu, J. Wang, H. Shi, and Z. Li, "Research on the radiation characteristics of the leaky coaxial cables," in *6th International Symposium on Antennas, Propagation and EM Theory*, 2003, pp. 242–245.

[15] S. Paulotto, P. Baccarelli, F. Frezza, and D. R. Jackson, "A novel technique for open-stopband suppression in 1-D periodic printed leaky wave antennas," *IEEE Transactions on Antennas and Propagation*, vol. 57, no. 7, pp. 1894–1906, 2009.

[16] W. Zhou, J. Liu, and Y. Long, "Applications of the open-stopband suppression in various periodic leaky-wave antennas with tapered half wavelength line," *IEEE Transactions on Antennas and Propagation*, vol. 67, no. 11, pp. 6811–6820, 2019.

[17] S. O. Kamal and L. B. Lok, "Array of coaxial periodic leaky wave antennas in parallel configuration for restricted volume applications," in *IEEE International Symp. on Antennas and Propagation and USNC-URSI Radio Science Meeting*, 2023, pp. 199–200.

[18] C. A. Balanis, Antenna theory: analysis and design. John Wiley & Sons, 2016.

[19] Y. Geng *et al*., "A leaky-wave antenna array with beam-formed radiation pattern for application in a confined space," *IEEE Access*, vol. 7, pp. 86 367–86 373, 2019.

[20] D. K. Karmokar, K. P. Esselle, and T. S. Bird, "An array of half-width microstrip leaky-wave antennas radiating on boresight," *IEEE Antennas and Wireless Propag. Letts.*, vol. 14, pp. 112–114, 2015.

[21] M. Alibakhshikenari *et al*., "High-isolation leaky-wave array antenna based on CRLH-metamaterial implemented on SIW with ±30° frequency beam-scanning capability at millimetre-waves," *Electronics*, vol. 8, no. 6, 2019.